2011

Analysis of Fracture Energy: Comparative Study of PCC & FRC

Yi-Cheng Chiu
Parth Panchmatia
Aswathy Sivaram
Purdue University
4/27/2011

Table of Contents

List of Figures and Tables

Chapter 1: Introduction

1 Introduction

1.1 Introduction

It is a well known fact that concrete is a brittle material. It shows great compressive strength values but under tension it fails suddenly at much lower loads. To prevent catastrophic failures of concrete structures, designers introduce steel reinforcements in regions where the structure is expected to be under tension.

Another attempt to prevent catastrophic failure of concrete under tensile stresses is the introduction of fibers in the matrix of concrete. These fibers prevent crack growth and thus increase the ductility of concrete. Therefore it would be interesting to study the effect of inclusion of fibers in concrete on the fracture energy and crack growth pattern.

In this project, we cast concrete with and without fibers. To make sure that we eliminate any other variability and just account for the effect of fibers in our results, we keep the mix designs for both concretes exactly similar. We add 1.2% by volume of steel fibers in concrete.

Specimens prepared are tested for 7-day compressive strength and four-point bending. By attaching an LVDT to the center point of the beam, we obtain the load displacement plots for both plain concrete and fiber reinforced concrete. We use these plots to calculate the fracture energy using Hillerborg and Jenq-Shah (Two Parameter Fracture) models.

Chapter 2: Experiment

2 Experimental Design, Setup and Results

2.1 Specimen Preparation

2.1.1 Mix Design

The main aim of this project was to study the effect of inclusion of fibers on the fracture energy and toughness of concrete. So, to ensure that there are no other variations we kept the mix designs exactly the same with just the exception of adding fibers in the second mix. The mix designs are presented in Table 1(plain concrete) and Table 2 (fiber reinforced concrete).

Table 1: Mix Design for Plain Cement Concrete

Plain Concrete		
Materials	Weight (lb/cu yd)	Weight (lb/batch)
Cement	515.0	19.1
Sand	1400.0	51.8
Recycled Concrete Aggregates	1600.0	57.9
Water	216.5	9.46
Air entraining Agent	0.5 oz	2.8 ml
Water Reducing Agent	2.5 oz	14 ml
w/c	0.42	0.42

Table 2: Mix Design for Fiber Reinforced Concrete

Fiber Reinforced Concrete		
Materials	Weight (lb/cu yd)	Weight (lb/batch)
Cement	515.0	19.1
Sand	1400.0	51.8
Recycled Concrete Aggregates	1600.0	57.9
Water	216.5	9.46
Air entraining Agent	0.5 oz	2.8 ml
Water Reducing Agent	2.5 oz	14 ml
w/c	0.42	0.42
Steel Fibers	1.2 % by Volume	5.88

These mix designs are designed for Saturated Surface Dry (SSD) conditions and therefore the water added in the batch will give a greater w/c ratio than 0.42 which will yield w/c

ratio of 0.42 once the aggregate moisture corrections are accounted for. The batch size for both mixes was 1 cu ft.

The mixing sequence for plain concrete and FRC are presented in Table 3 and Table 4.

Table 3: Mixing sequence for Plain Cement Concrete

Sr. No.	Activity	Time
1.	Adding coarse and fine aggregates and mixing it with some mix water	0 – 1 min
2.	Adding cement and the remaining water and mixing it for three minutes. During this time the air entraining agent and the water reducer are also added.	1 – 4 min
3.	Dormant Period	4 – 7 min
4	Second round of mixing	7 – 12 min

Table 4: Mixing Sequence for Fiber Reinforced Concrete

Sr. No.	Activity	Time
1.	Adding coarse and fine aggregates and mixing it with some mix water	0 – 1 min
2.	Adding cement and the remaining water and mixing it for three minutes. During this time the air entraining agent and the water reducer are also added.	1 – 4 min
3.	Dormant Period	4 – 7 min
4	Second round of mixing with **addition of steel fibers**	7 – 12 min

2.1.2 Casting

Five beams of dimension 3”x 4” x 16” were cast for each mix in addition to the three cylinders. All of these were cast in two layers and each layer was vibrated on a vibrating table for 30 seconds. In case of FRC, finishing the moulds became less workable, so we had to vibrate it for one minute.

2.2 Compressive Strength

The compressive strength testing was carried out in accordance with ASTM C 39. To summarize this, the size of the cylinders to be used should be eight inch in length and 4 inch in diameter. The rate of loading should be maintained at 35psi/s until failure. The compressive strength test results are summarized in Table 5.

Table 5: Compressive Strength

Sr. No	PCC (psi)	FRC (psi)
1	4155	4280
2	4345	4230
3	4360	4216
Average	4287	4242

The inclusion of steel fibers does not alter the compressive strength values much. Therefore, for all calculations henceforth, we will use 30MPa (4350 psi) as compressive strength.

2.3 Four Point Bending Test

2.3.1 Experimental Setup

Figure 2.1 shows the experimental setup used to obtain the load-displacement data from the data acquisition system. The length of the beam is sixteen inches, the breath is four inches and the height is three inches. The bottom supports are placed one inch from the edge of the specimen and the loading apparatus is placed at the center of the beam. Hence the span is 14 inches. The space between the two loading points is three inch. A LVDT is placed on the center of the beam behind the beam. Similar set-up was used for testing both plain concrete and fiber reinforced concrete.

The load-displacement plot obtained for plain concrete and fiber reinforced concrete are shown in Figure 2.2 and Figure 2.3 respectively.

Figure 2.1: Experimental Setup for four point bending test

2.3.2 Results

Figures 2.2, 2.3 and 2.4 show the Load versus Displacement plots for the specimens tested. Fig 2.2 shows the results for plain cement concrete, Fig 2.3 is the plot for FRC and Fig 2.4 is the plot for plain concrete with 1.25'' notch depth. The values are the averages of data from 3 sets of specimens each. From Figure 2.2 and Figure 2.3, we can notice the following.

1. The peak load for PCC and FRC do not differ much
2. FRC deflects by 25mm as opposed to a 2mm deflection for PCC before complete failure.

This shows us that, even though the low volume addition of fibers (1.2% by volume) in concrete does not alter the tensile strength, the ductility increases significantly.

In case of a notched specimen, we notice that the peak load reduces significantly (Fig. 2.4). As expected, the deformation value is also less compared to un-notched specimen.

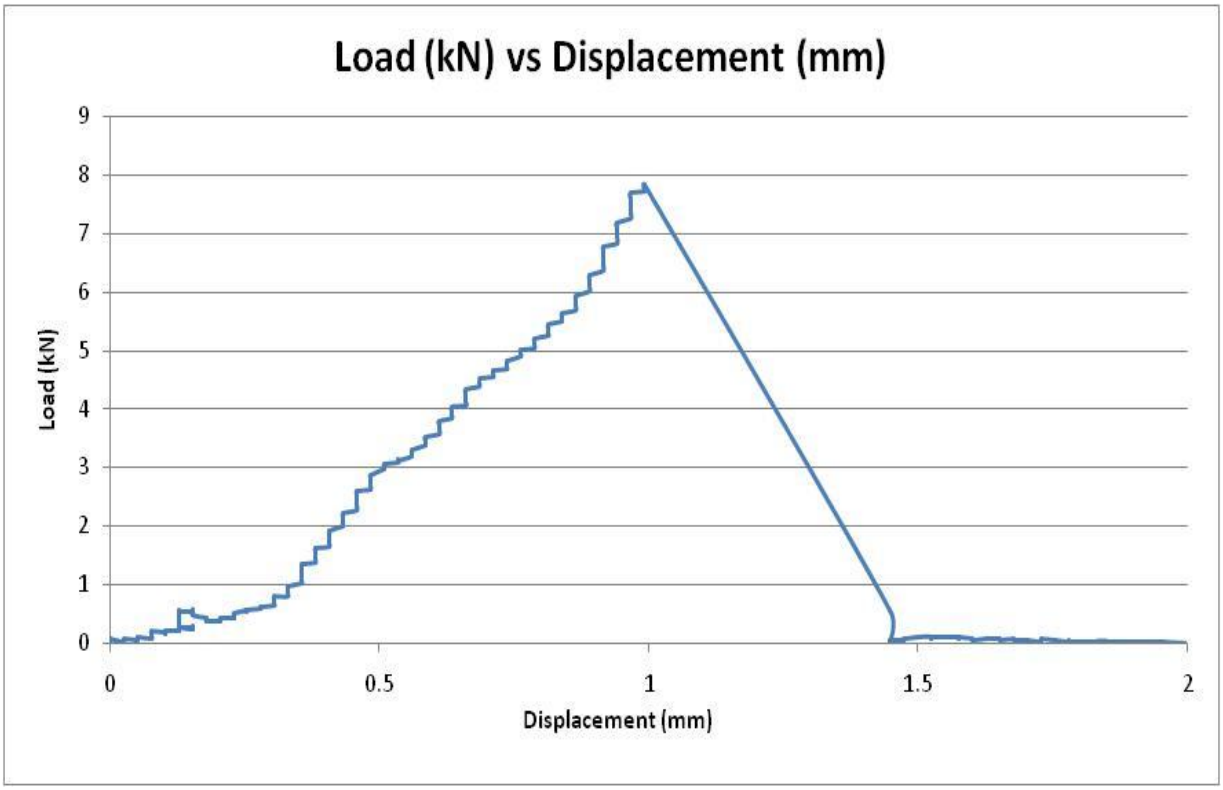

Figure 2.2: Load Displacement Curve for Plain Cement Concrete

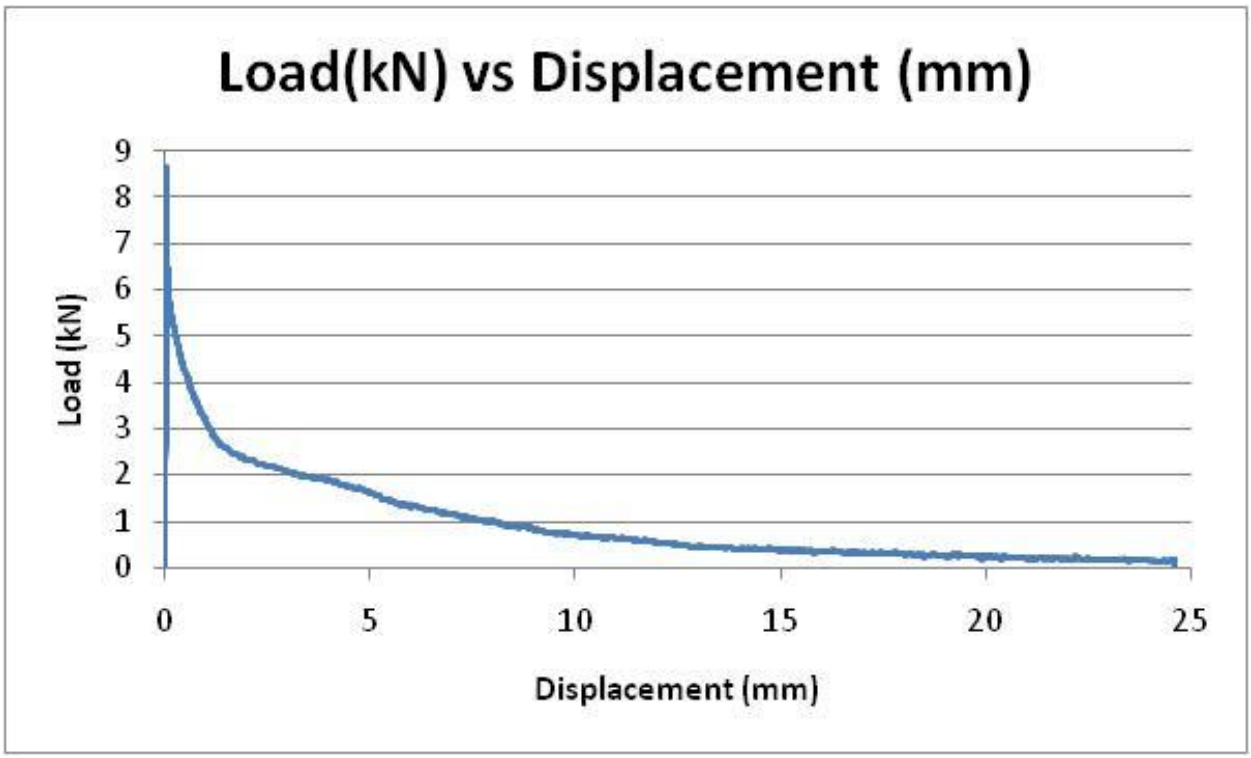

Figure 2.3: Load Displacement Curve for Fiber Reinforced Concrete

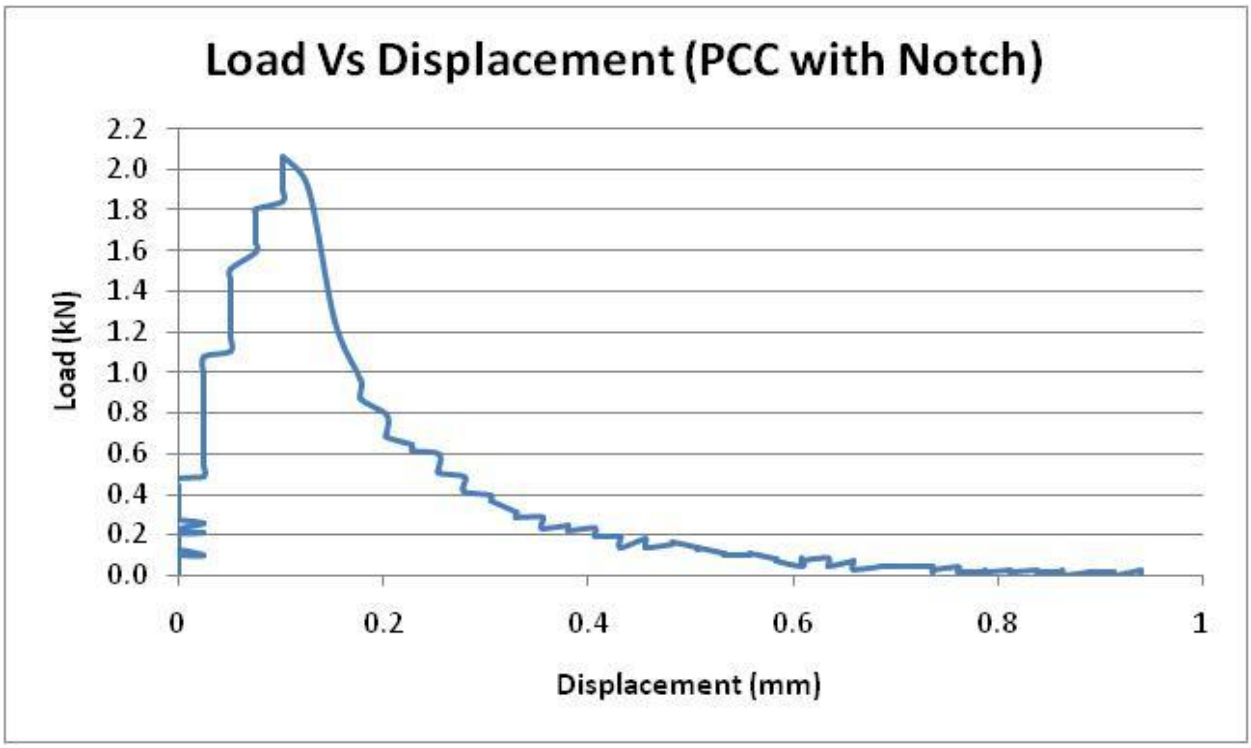

Figure 2.4: Load Displacement Curve for Plain Concrete Specimen with Notch

Figures 2.5 – 2.7 shows the grack growth in the fiber reinforced specimen, and crack propagation and ultimately failure of the specimen.

Figure 2.5: Photograph Showing Crack Growth in FRC

Figure 2.6: Photograph Showing Various Crack Paths in FRC

Figure 2.7: Photograph Showing Fracture Surfaces for FRC after Complete Failure. Failure occurs due to pullout of fibers from the concrete matrix.

Chapter 3: Analysis using models

3 Theoretical Analysis

3.1 Hillerborg Model

The most direct way of determining the specific fracture energy, GF, is by means of a uniaxial tensile test, where the complete stress-deformation curve is measured. However, it is difficult to perform the tensile test so Hillerborg's model adopts an indirect method: the three point bend test on a beam (Fig. 3.1) (Hillerborg, 1985).

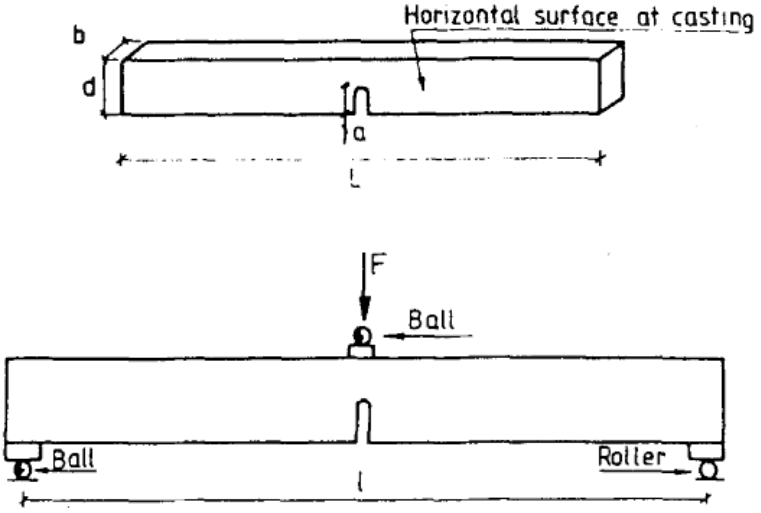

Figure 3.1: Proposed Standard Test Beam for G_F tests (Hillerborg, 1985)

The general idea of this type of test is to measure the amount of energy which is absorbed when the specimen is broken into two halves. This energy is divided by the fracture area (projected on a plane perpendicular to the tensile stress direction). The resulting value is assumed to be the specific fracture energy GF.

During the test, the beam is acted upon not only the imposed load from machine but also by the weight of beam itself and the testing equipment. Consequently the measured load-deflection curve does not give the total amount of absorbed energy. Hence, a correction must be made for the weight of the beam (Petersson, 1981). Figure 3.2 shows a load-deflection curve.

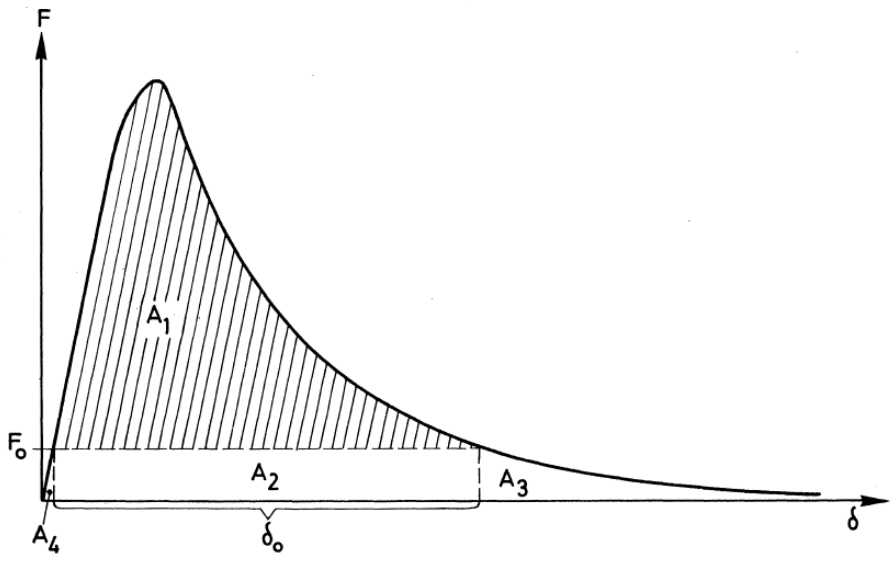

Figure 3.2: A load-deflection curve for a stable three point bend test on a notched beam.

The shaded area (A1) in Fir 3.2 defines the area under the load-deflection curve if there is no correction for the energy supplied by the weight of the beam (Petersson, 1981). F is the force or the load, δ is the central deflection of test beam, and the area under the curve is the absorbed energy. The specific fracture energy GF can be obtained as:

$$G_F = \frac{\mathrm{A}}{\mathrm{b(d-a)}}$$

where a is the length of the notch, b is the thick of the beam, and d is the depth of the beam (Fig. 3.1). The total amount of absorbed energy A is:

$$A=A_1+A_2+A_3+A_4$$

A_1 is the area below the measured load-deformation curve. $A_2 = F_0\delta_0$, where δ_0 is the deformation when F=0 and the beam breaks. The additional load F_0 is the central load, which gives rise to the same central bending moment as the weight of the beam and the testing equipment, which is not included in the measured load F. F_0 can be found by equating the moment due to F_0 and the moment due to the weight of the beam:

$$\frac{\mathrm{F}_0 l}{4} = \frac{\mathrm{mg}l^2}{8}$$

So,

$$F_0 = \frac{mgl}{2} = \frac{Mg}{2}$$

where m = weight per unit length of the beam, M = weight of the beam (between the supports) and g = 9.81 m/s^2.

It can be demonstrated that A_3 is approximately equal to A_2, and normally A_4 is so small (less than 1-2% of the total area) that it can be neglected (Petersson, 1981). Thus the total amount of absorbed energy can be taken as:

$$A = A_1 + 2F_0\delta_0$$

Then, the specific fracture energy G_F of Hillerborg's model can be obtained as

$$G_F = \frac{A_1 + Mg\delta_0}{b(d-a)}$$

3.2 Two Parameter Model

In 1985, Jenq and Shah (Jenq, 1985) proposed the Two-Parameter Fracture Method (TPFM), accounting for the precritical crack growth that occurs prior to the peak load (Jansen, 2001). When fracture toughness is evaluated from notched specimens using conventional LEFM (measured peak load and initial notch length) a significant size effect is observed. This size effect has been attributed to nonlinear slow crack growth occurring prior to the peak load. The TPFM takes into account this non-linearity in crack growth. Critical stress intensity factor, K_{IC}, is calculated at the tip of the effective crack. The critical effective crack extension is dictated by the elastic critical crack tip opening displacement, CTODc. Therefore, this is a critical crack model in which the length of the stable crack growth at peak is determined to account for non-linearities in the system.

This model asserts that the global response of a structure with a crack experiencing NLFM conditions can be reproduced by considering the structure to have an effective crack experiencing LEFM conditions. This can be expressed by substituting the effective critical crack length, a_c. To perform analysis with this model, the notched specimen is loaded and the compliance of the load versus crack mouth opening displacement, which is called the initial compliance and denoted by C_i is determined. Using C_i and initial crack length a_o, which is the depth of the notch, the modulus of elasticity E is calculated. Then we proceed to determine the length of the effective critical crack, a_c, which the length of the crack that occurs at the peak load. Using a_c and the unloading compliance at

peak load C_u, and some additional parameters, the fracture toughness, K_{IC} can be obtained. Fig. 3.3 illustrates the initial and unloading compliance as seen in a load versus CMOD curve.

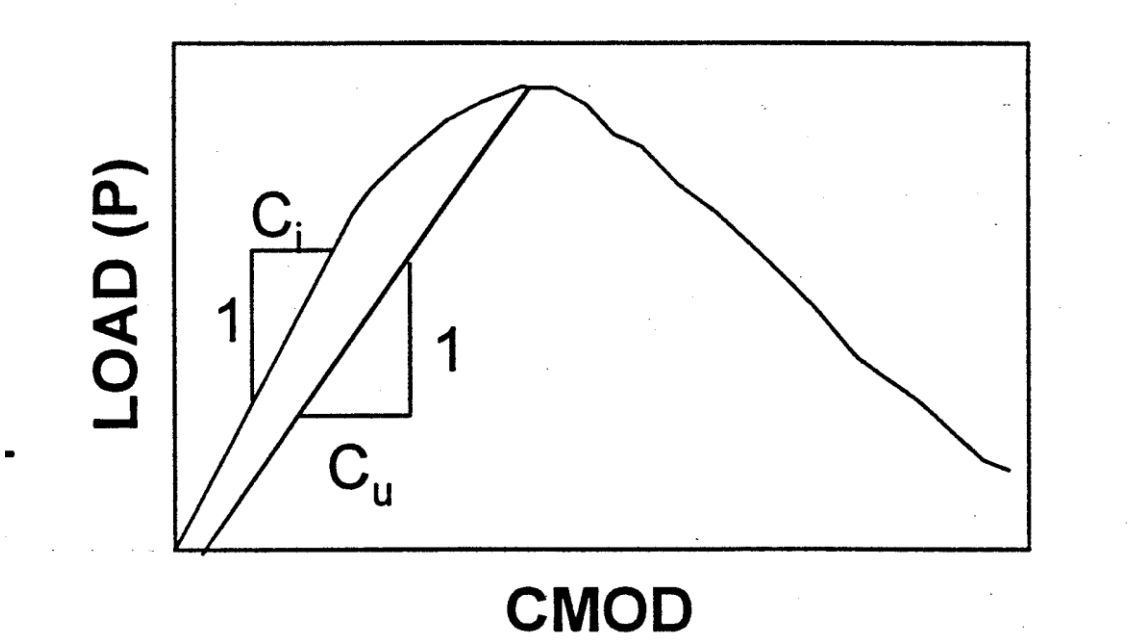

Figure 3.3: Illustration of TPFM: Determination of Fracture Toughness from Load vs. CMOD curve (Jansen, 2001)

The equations used to determine K_{IC} from experimental data are as follows.
The modulus of elasticity from the beam test is given by

$$E = \frac{6Sa_0V_1(\alpha)}{C_i b h^2}$$

and,

$$V_1(\alpha) = 0.76 - 2.28\alpha + 3.87\alpha^2 - 2.04\alpha^3 + \frac{0.66}{(1-\alpha)^2}$$

Where:

S = specimen span length
b=specimen width
h=specimen depth
a_0=initial notch length
$\alpha = a_0/h$
C_i=initial compliance from Load vs. CMOD

In our case, since a_0=0 (un-notched specimens), we use the ASTM standard equation using compressive strength to compute E.

$$E = 57000\sqrt{f_c'}$$

Note that f_c' is in psi.
To determine the effective critical crack length, the following equation is used.

$$a_c = \frac{EC_u bh^2}{6SV_1(\alpha_c)}$$

Where:

$\alpha_c = a_c/h$

Cu=unloading compliance from the Load vs. CMOD curve

The fracture toughness is calculated at the peak load using

$$K_{IC} = \frac{6Y(\alpha)M_c\sqrt{a_c}}{bh^2}$$

where

$$Y(\alpha) = \frac{1.99 - a_c(1-a_c)(2.15 - 3.93a_c + 2.7a_c^2}{(1+2a_c)(1-a_c)^{\frac{3}{2}}}$$

and,

$$M_c = P_c\frac{S}{4} + p\frac{S^2}{8}$$

Where:

P_c = Peak load

p = Distributed load due to self weight of the beam

From these values, the fracture energy can be computed as

$$G = \frac{K_{IC}^2}{E}$$

Chapter 4: Results

4 Results from Hillerborg and Two Parameter Model

4.1 Hillerborg Model

We calculated the fracture energy, for the average load vs. displacement curve obtained from five each of plain cement concrete and steel fiber reinforced concrete specimens. For the PCC specimens without notch, the fracture energy was 0.528 N/mm. For the notched specimen, the fracture energy was lesser, 0.1 N/mm. This is because in notched specimens, crack is located very close to the notch plane, and hence non-linear deformations are absent in the rest of the specimen and all the energy spent could be attributed to crack growth (Giaccio, 2008).

For the FRC specimens, without notch, the fracture energy was found to be 2.815 N/mm. Displacement data for the notched specimen was not available, since during the test, the LVDT lost contact with the specimen. We see that there is around 400% increase in fracture energy of FRC, compared to that of PCC. This is expected, as the steel fibers added to the system introduce ductility, and concrete which is quasi-brittle in nature, acts like a ductile material.

4.2 Two Parameter Fracture Model

For the same average load vs. displacement curve, we linearized the CMOD values using the following equation:

$$\theta = \frac{l\delta}{2}$$

$$CMOD = 2h\theta$$

To use the above equation, we assume that the specimen follows rigid body rotation, both in the case of PCC and FRC. Fig. 3.4 shows the specimen geometry corresponding to the CMOD and vertical displacement.

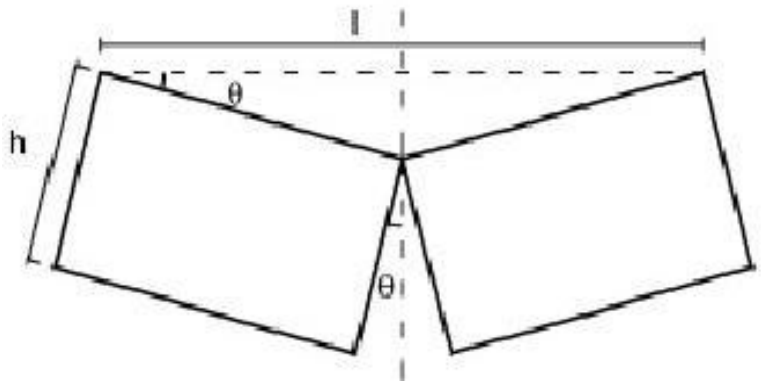

Figure 4.1: Illustration of specimen geometry for calculating CMOD from vertical displacement data

Using this CMOD value, we generated the load vs. CMOD curve, and obtained the initial compliance. Since unloading test was not performed, we approximated the unloading compliance Cu to be same as the initial compliance, Ci. This was also because Cu and Ci data from literature (Jansen, 2001) were almost similar. We then used the equations given in section 3.2 to obtain fracture energy values.

For the PCC specimens without notch, the fracture energy was 0.557 N/mm. This data is in accordance with the fracture energy obtained from Hillerborg method.

For the FRC specimens, without notch, the fracture energy was found to be 0.17 N/mm. This value is very unrealistic, since we expect the fibers to introduce ductility, and hence the fracture energy should be higher than that of PCC.

Chapter 5: Discussion

5 Discussion

The two parameter model gave unrealistic values for the fracture energy of FRC, as compared to that of the Hillerborg model. In the analysis of results, let us take a look at the assumptions that we make to follow the analysis.

We use the following assumptions in our analysis.

1. Rigid body rotation holds for FRC beam.
2. CMOD is a linear function of vertical displacement.
3. No actual unloading data, Cu approximated as the slope of the linear elastic region.
4. All data from un-notched specimens, but analysis is given for notched specimens.

Since FRC is much more ductile and does not follow rigid body rotation in reality, the assumption does not hold, and hence it cannot be correlated linearly to the vertical displacement data. Also, theories for notched specimens were modified to fit un-notched data (by neglecting notch depth). This also requires some further investigation.

The major reason for the deviation of fracture energy obtained from the TPFM is because this model does not consider post peak behavior of the FRC load vs. displacement curve. The TPFM does not consider the area under the load-displacement curve. There is not much difference in the peak loads of PCC and FRC. The difference occurs in the post-peak behavior. Almost all of the contribution to the fracture energy of the FRC specimen comes from the area under the curve after the peak load. The TPFM considers data only up to the peak load, and this gives values of lower magnitude for the fracture energy. This deems the Two Parameter model unfit for use in calculating fracture toughness of FRC specimens. Further investigation is required to come up with correction factors for this model.

Chapter 6: Conclusions and Future Work

6 Conclusions and Future Work

6.1 Conclusions

We conducted four point bending experiments of five sets of PCC and FRC specimens at 7 day strength. We compared fracture energy values obtained using Hillerborg model and Two Parameter Fracture model. For PCC, both the models gave very similar values. But for FRC, the two parameter model gave unrealistic values. Almost all of the contribution to the fracture energy of the FRC specimen comes from the area under the load-displacement curve after the peak load. The TPFM considers data only up to the peak load, and this gives values of lower magnitude for the fracture energy. This deems the Two Parameter model unfit for use in calculating fracture toughness of FRC specimens. Further investigation is required to come up with correction factors for this model.From our studies, we conlcude that the two parameter model is ineffective for calculating fracture energy in steel fiber reinforced concrete. We have made a few assumptions to suit the models based on our experimental data. The applicability of these assumptions need to be studied in depth. Further investigation is required to come up with correction factors for the two parameter model to enable FRC fracture energy predictions.

6.2 Future Work

We suggest that further experimentation be conducted using LVDTs to measure the CMOD directly. Experimentation may also benefit from a slower loading rate in case of FRC specimens, to avoid any dynamic changes in elastic properties of the concrete. Also, using a closed-loop servo-hydraulic machine to obtain unloading data for calculating compliance is also significant. This will give experimental data for the initial and unloading compliances, using which the fracture energy can be computed with higher accuracy.

References

7 References

Giaccio, G. T. (2008). Use of small beams to obtain design parameters of fiber reinforced concrete. *Cement & Concrete Composites* , 297-306.

Hillerborg, A. (1985). The theoretical basis of a method to determine the fracture energy GF of concrete. *Mater. Struct. , 18* (4), 291-296.

Jansen, D. C. (2001). Simplification of the Testing and Analysis Procedure for the Two Parameter Fracture Model. *CI-SP 201, Fracture Mechanics for Concrete Materials: Testing and Applications* , 17-34.

Jenq, Y. a. (1985). Two Parameter Fracture Model for Concrete. *Journal of Engineering Mechanics , 111* (10), 1227-1241.

Petersson, P. (1981). Crack growth and formation of fracture zones in plain concrete and similar materials. *Report-I-VBM-1006* .